

## Articles

Synthesis and Structural Characterization of a Fluorinated  $\alpha$ -Diimine Platinum(II) ComplexMartin Lersch,<sup>§</sup> Alexander Krivokapic, and Mats Tilset\*

Department of Chemistry, University of Oslo, P.O. Box 1033 Blindern, N-0315 Oslo, Norway

Received September 29, 2006

The preparation of an electron-deficient (N–N)PtCl<sub>2</sub> complex in which the diimine C is substituted by CF<sub>3</sub> is described. Thus, reactions between the diimine ligand **1** (R = CF<sub>3</sub>, R' = 2,6-dimethylphenyl) and PtCl<sub>2</sub> (thermal reaction) or KPtCl<sub>3</sub>(C<sub>2</sub>H<sub>4</sub>) (photochemically activated) furnishes the corresponding (N–N)PtCl<sub>2</sub> complex **2**. The ligand **1** and its Pt complexes **2**, as well as related (N–N)PtCl<sub>2</sub> complexes **3** (R = CO<sub>2</sub>CD<sub>3</sub>, R' = 2,6-dimethylphenyl; a methanolysis product) and **4** (R = H, R' = 2,6-dimethylphenyl) have been characterized by X-ray crystallography.

## Introduction

Metal complexes with 1,4-diaza-1,3-butadiene ligands<sup>1,2</sup> (N–N = R'N=C(R)C(R)=NR'; R' = alkyl, aryl), which belong to the class of  $\alpha$ -diimine ligands, have inspired considerable research efforts. For example, such complexes have found widespread use in efficient olefin polymerization catalysts<sup>3,4</sup> and in C–H bond activation reactions.<sup>5–7</sup> The interesting photochemical and photophysical properties of such compounds have also been thoroughly investigated.<sup>8</sup> The substituent R at the imine carbon is most commonly a hydrogen atom or an alkyl or aryl group. These  $\alpha$ -diimines are usually prepared by condensation of primary amines or anilines with 1,2-diones (R = alkyl, aryl) or glyoxal (R = H). The strong  $\pi$ -acceptor ability that results from a rather low-lying  $\pi^*$  LUMO is a characteristic feature of the  $\alpha$ -diimine systems.<sup>9</sup> This property greatly influences the structure and reactivity of  $\alpha$ -diimine metal coordination compounds.<sup>2</sup> Semiempirical calculations have shown that the introduction of R = perfluoroalkyl, perfluoroaryl groups should further lower the LUMO and further enhance the  $\pi$ -acceptor ability of the ligands.<sup>10</sup> This would render the metal center of their complexes more electron deficient, with possibly

significant consequences for the mechanistic features and inherent reactivities of diimine–Pt complexes in C–H activation chemistry.<sup>7</sup>

There have been a limited number of reports that describe the incorporation of R = perfluoroalkyl groups in  $\alpha$ -diimines. Diel et al.<sup>10</sup> prepared  $\alpha$ -diimines with R = CF<sub>3</sub>, C<sub>6</sub>F<sub>5</sub>, R' = SiMe<sub>3</sub> from perfluorobiacetyl and decafluorobenzil, respectively. Uneyama and co-workers<sup>11,12</sup> synthesized a variety of  $\alpha$ -diimines with R = CF<sub>3</sub>, C<sub>3</sub>F<sub>7</sub>, R' = 4- and 2,6-substituted phenyl employing a CO-promoted Pd-catalyzed homocoupling of fluorinated imidoyl iodides. An alternative approach was presented by Sadighi et al.,<sup>13</sup> starting from an analogous fluorinated imidoyl iodide but using SmI<sub>2</sub> as the reductive coupling reagent (R = CF<sub>3</sub>, R' = 3,5-(CF<sub>3</sub>)<sub>2</sub>C<sub>6</sub>H<sub>3</sub>). Finally, Diel et al. recently described the reductive coupling of perfluoroalkyl and perfluoroaryl cyanides with [Cp<sub>2</sub>TiCl]<sub>2</sub> followed by protonolysis to liberate the formed  $\alpha$ -diimines (R = CF<sub>3</sub>, C<sub>6</sub>F<sub>5</sub>, R' = H).<sup>14</sup>

Despite the aforementioned reports of  $\alpha$ -diimines with perfluorinated hydrocarbyl groups at the diimine “backbone” positions, the only metal complex of such diimines known to date is a species in which a Pd(PPh<sub>3</sub>)<sub>2</sub> moiety is presumed to be coordinated in an  $\eta^2$ (C,N) fashion to one imine.<sup>13</sup> This complex was not isolated and thence not structurally characterized; its structure was proposed solely on the basis of <sup>31</sup>P and <sup>19</sup>F NMR spectra, which indicated nonequivalence of the halves of the diimine ligand and two nonequivalent phosphines. Metal chelate complexes of the fluorinated diimines have not yet been described.

In this contribution we present thermal and photochemical pathways to (N–N)PtCl<sub>2</sub> (**2**; N–N = R'N=C(R)C(R)=NR' with R = CF<sub>3</sub>, R' = 2,6-Me<sub>2</sub>C<sub>6</sub>H<sub>3</sub>) together with X-ray structures of the ligand **1**, the complex **2**, a methanolysis product

\* To whom correspondence should be addressed. E-mail: mats.tilset@kjemi.uio.no.

<sup>§</sup> Present address: Borregaard Ind. Ltd., P.O.B. 162, N-1701 Sarpsborg, Norway.

(1) tom Dieck, H.; Svoboda, M.; Greiser, T. *Z. Naturforsch., B* **1981**, *36B*, 823–832.

(2) van Koten, G.; Vrieze, K. *Adv. Organomet. Chem.* **1982**, *21*, 151–239.

(3) Ittel, S. D.; Johnson, L. K.; Brookhart, M. *Chem. Rev.* **2000**, *100*, 1169–1203.

(4) Gibson, V. C.; Spitzmesser, S. K. *Chem. Rev.* **2003**, *103*, 283–315.

(5) Stahl, S. S.; Labinger, J. A.; Bercaw, J. E. *Angew. Chem., Int. Ed.* **1998**, *37*, 2181–2192.

(6) Fekl, U.; Goldberg, K. I. *Adv. Inorg. Chem.* **2003**, *54*, 259–320.

(7) Lersch, M.; Tilset, M. *Chem. Rev.* **2005**, *105*, 2471–2526.

(8) van Slageren, J.; Klein, A.; Zalis, S. *Coord. Chem. Rev.* **2002**, *230*, 193–211.

(9) Reinhold, J.; Benedix, R.; Birner, P.; Hennig, H. *Inorg. Chim. Acta* **1979**, *33*, 209–213.

(10) Diel, B. N.; Deardorff, P. J.; Zelenski, C. M. *Tetrahedron Lett.* **1999**, *40*, 8523–8527.

(11) Amii, H.; Kohda, M.; Seo, M.; Uneyama, K. *Chem. Commun.* **2003**, 1752–1753.

(12) Uneyama, Kenji, Amii, Hideki, and Koda, Mitsuhiro. Jpn. Patent 2001253861, 2001.

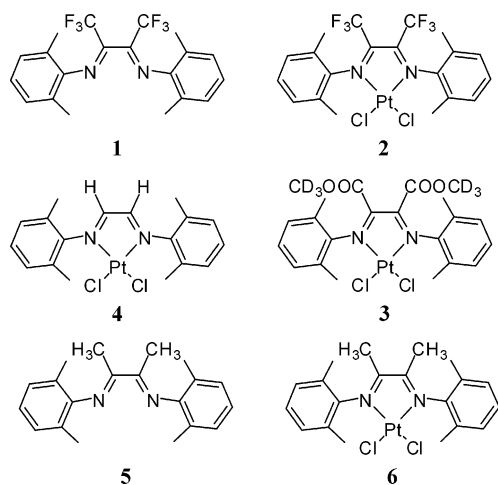
(13) Sadighi, J. P.; Henling, L. M.; Labinger, J. A.; Bercaw, J. E. *Tetrahedron Lett.* **2003**, *44*, 8073–8076.

(14) Diel, B. N.; Deardorff, P. J.; Zelenski, C. M.; Incarvito, C.; Liable-Sands, L.; Rheingold, A. M. *Inorg. Chim. Acta* **2004**, *357*, 3902–3910.

**3** (R = CO<sub>2</sub>CD<sub>3</sub>) that is derived from **2**, and the related Pt complex **4** (R = H, R' = 2,6-Me<sub>2</sub>C<sub>6</sub>H<sub>3</sub>), which is of interest for comparison of certain structural features found in **2** and **3**.

## Results

**1. Preparative Work.** Attempts at metalating the  $\alpha$ -diimine ligand **1** to furnish **2** under thermal conditions with (SMe<sub>2</sub>)<sub>2</sub>-PtCl<sub>2</sub> and KPtCl<sub>3</sub>(C<sub>2</sub>H<sub>4</sub>) (Zeise's salt) in toluene or methanol were unsuccessful. This is in line with previous observations.<sup>13</sup>



At ambient temperature, no reactions were detected by <sup>1</sup>H or <sup>19</sup>F NMR; prolonged heating decomposed the Pt precursors to Pt black. Similarly, attempts at using microwave heating and medium pressures (<10 bar) failed, producing Pt black within minutes. In water/methanol mixtures, K<sub>2</sub>PtCl<sub>4</sub> and **1** were soluble but decomposed to Pt black upon heating.

However, in one NMR sample of the ligand **1** and KPtCl<sub>3</sub>(C<sub>2</sub>H<sub>4</sub>) in methanol-*d*<sub>4</sub> which had only been moderately heated so that the starting materials remained mainly intact, dark crystals had formed after 6 months. These were indeed shown to be the desired product **2** by an X-ray diffraction analysis (vide infra), and this was the first indication that this product is not only accessible but also quite stable. A clue to what might have mediated the reaction was provided by the fact that the NMR sample had been exposed to indirect daylight.

Zeise's salt, known since 1827, continues to fascinate chemists.<sup>15</sup> Its photochemistry has been well studied and differs significantly from its thermal chemistry.<sup>16,17</sup> Inspired by this, we were gratified to find that attempts to facilitate the metalation of **1** with UV light from an 8 W chromatography UV lamp gave promising results. After 2 weeks of continuous irradiation of a methanol-*d*<sub>4</sub> solution of **1** and Zeise's salt in an NMR tube, crystals formed in the solution. However, these were identified as **3** by X-ray crystallography (vide infra) and are likely derived from **2** by methanolysis of the trifluoromethyl groups (Scheme 1). Characteristic <sup>19</sup>F peaks appeared and later disappeared in the <sup>19</sup>F NMR spectra during the course of the reaction, signaling the presence of unidentified intermediates. Hydrolysis of trifluoromethyl groups has been described<sup>18,19</sup> and is also known

(15) Benedetti, M.; Fanizzi, F. P.; Maresca, L.; Natile, G. *Chem. Commun.* **2006**, 1118–1120.

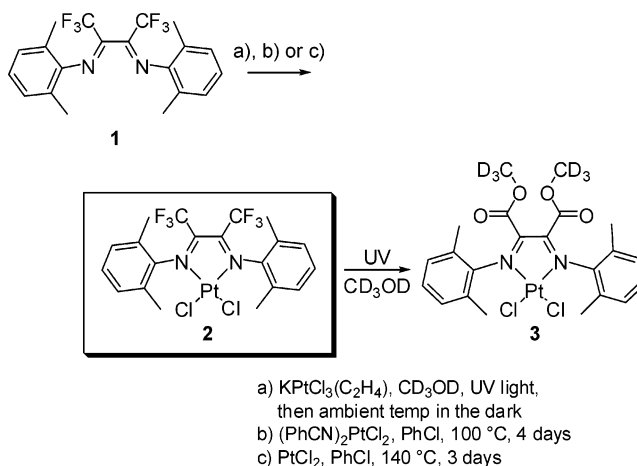
(16) Natarajan, P.; Adamson, A. W. *J. Am. Chem. Soc.* **1971**, *93*, 5599–5605.

(17) Adamson, A. W.; Fleischauer, P. D., Eds. *Concepts of Inorganic Photochemistry*; Wiley: New York, 1975.

(18) Kimoto, H.; Cohen, L. A. *J. Org. Chem.* **1979**, *44*, 2902–2906.

(19) Kobayashi, Y.; Kumadaki, I. *Acc. Chem. Res.* **1978**, *11*, 197–204.

## Scheme 1<sup>a</sup>



- a) KPtCl<sub>3</sub>(C<sub>2</sub>H<sub>4</sub>), CD<sub>3</sub>OD, UV light, then ambient temp in the dark  
 b) (PhCN)<sub>2</sub>PtCl<sub>2</sub>, PhCl, 100 °C, 4 days  
 c) PtCl<sub>2</sub>, PhCl, 140 °C, 3 days

<sup>a</sup> Legend: (a) KPtCl<sub>3</sub>(C<sub>2</sub>H<sub>4</sub>), CD<sub>3</sub>OD, UV light, then ambient temperature in the dark; (b) (PhCN)<sub>2</sub>PtCl<sub>2</sub>, PhCl, 100 °C, 4 days; (c) PtCl<sub>2</sub>, PhCl, 140 °C, 3 days.

to be facilitated by UV irradiation.<sup>20</sup> It should also be noted that some metallic Pt is deposited during the reaction, which also opens the possibility for Pt(0)-mediated C–F activation.<sup>21–23</sup>

An NMR tube containing equimolar amounts of **1** and Zeise's salt in methanol-*d*<sub>4</sub> which was exposed to 20 h of irradiation from the chromatography UV lamp furnished **2** as dark crystals in up to 48% yield, but only after standing in the dark for 15 weeks. We have not attempted a more elaborate study of the photochemistry of the system with more sophisticated photochemical equipment.

Zeise's anion quantitatively yields the solvento complex *trans*-PtCl<sub>2</sub>(C<sub>2</sub>H<sub>4</sub>)(CH<sub>3</sub>OH) in methanol solution.<sup>24</sup> Our results indicate that **1** does not thermally react with this species. On the basis of the observation that **2** is formed by a photochemical reaction and not by a thermal reaction from Zeise's salt, we speculate that photochemically generated<sup>16</sup> *cis*-PtCl<sub>2</sub>(CH<sub>3</sub>OH)(L), where L = CH<sub>3</sub>OH, C<sub>2</sub>H<sub>4</sub>, may be a crucial intermediate.

The primitive photochemistry experiments above established that **2** is indeed isolable and stable. In a search for Pt precursors thermally more robust than Zeise's salt or (SMe<sub>2</sub>)<sub>2</sub>PtCl<sub>2</sub>, we were intrigued by a report that (PhCN)<sub>2</sub>PtCl<sub>2</sub> had been reacted with unsymmetrical  $\alpha$ -diimines in chloroform or toluene at their reflux temperatures.<sup>25</sup> Accordingly, when **1** was stirred with an equimolar amount of (PhCN)<sub>2</sub>PtCl<sub>2</sub> for 3 days at 100 °C in chlorobenzene, ca. 25% conversion to the desired product **2** was seen. Unfortunately, excess (PhCN)<sub>2</sub>PtCl<sub>2</sub> could not be separated from **2**. Attempts to remove excess (PhCN)<sub>2</sub>PtCl<sub>2</sub> by reaction with 2,2'-bipyridyl resulted—not too surprisingly—in complete loss of the ligand **1** from **2**, presumably with the formation of (2,2'-bipyridyl)PtCl<sub>2</sub>.

Interestingly, the direct reaction of **1** with stoichiometric quantities of PtCl<sub>2</sub>—ironically, the simplest Pt(II) source conceivable for this chemistry—for 3 days in chlorobenzene at reflux

(20) Chaignon, P.; Cortial, S.; Guerineau, V.; Adeline, M. T.; Giannotti, C.; Fan, G.; Ouazzani, J. *Photochem. Photobiol.* **2005**, *81*, 1539–1543.

(21) Colmenares, F.; Torrens, H. *J. Phys. Chem. A* **2005**, *109*, 10587–10593.

(22) Jasim, N. A.; Perutz, R. N.; Whitwood, A. C.; Braun, T.; Izundu, J.; Neumann, B.; Rothfeld, S.; Stammler, H.-G. *Organometallics* **2004**, *23*, 6140–6149.

(23) Hofmann, P.; Unfried, G. *Chem. Ber.* **1992**, *125*, 659–661.

(24) Plutino, M. R.; Otto, S.; Roodt, A.; Elding, L. I. *Inorg. Chem.* **1999**, *38*, 1233–1238.

(25) Yang, K.; Lachicotte, R. J.; Eisenberg, R. *Organometallics* **1997**, *16*, 5234–5243.

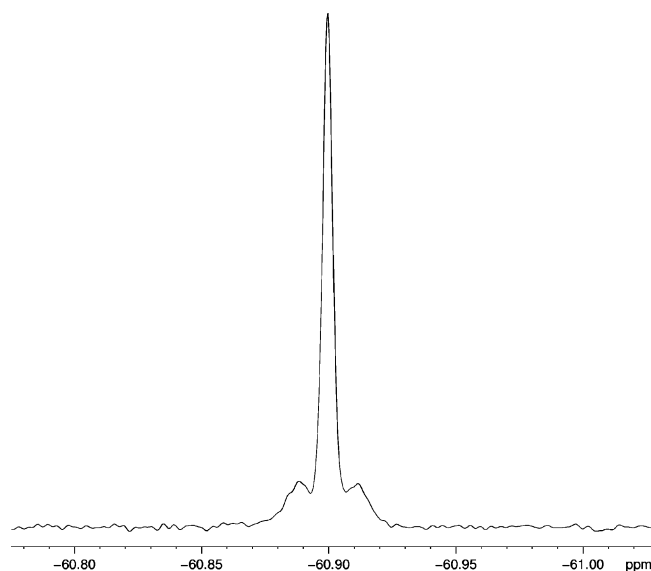


Figure 1.  $^{19}\text{F}$  NMR spectrum of **2** with coupling  $^4J_{\text{Pt-F}} = 4.4$  Hz.

under an atmosphere of  $\text{N}_2$  gave pure **2** in 11% yield (Scheme 1, reaction c). Excess ligand could easily be removed with pentane, and excess  $\text{PtCl}_2$  was removed by centrifugation or by filtration of a dichloromethane solution of the crude product through Celite. The unreacted starting materials could be recovered and resubmitted to the reaction conditions, giving another crop of product for a combined 19% yield.

The reactivity of  $\text{PtCl}_2$  toward electron-deficient **1** came as a surprise to us, despite previous reports of direct reactions with less electron-deficient diimine ligands.<sup>26</sup> The diimine ligand **1** and the product **2** show a remarkable stability, even after several days in refluxing chlorobenzene.

**2. Spectroscopic Characterization.** Complete spectroscopic and characterization data for all new compounds in this study are provided in the Experimental Section. Only some notable features are highlighted in the following.

The fluorinated ligand **1** displays two broad signals with different intensities for the N-aryl methyl signals in the  $^1\text{H}$  ( $\delta$  1.54 and 2.08; 1:0.83 intensity ratio) and for the  $\text{CF}_3$  groups in the  $^{19}\text{F}$  ( $\delta$  -66.1 and -68.4) NMR spectra. This may be caused by the coexistence of *E* and *Z* configurations relative to the  $\text{C}=\text{N}$  bonds (see Discussion). At elevated temperatures in toluene- $d_8$ , the  $^1\text{H}$  NMR spectra of **1** underwent gradual and reversible changes so that the two N-aryl methyl peaks underwent coalescence at ca. 70 °C. Conversely, gradual cooling to -80 °C resulted in sharpening, splitting, and further broadening of peaks, indicative of the intervention of several unidentified dynamic processes. Interestingly, only **1** and the related  $\text{R}' = 2,6\text{-iPr}_2\text{C}_6\text{H}_3$  substituted ligand system have been reported to exhibit such behavior, whereas ligands with  $\text{R}' = 4$ -substituted aryl groups show the expected NMR spectra that indicate simple, symmetrical diimines with no discernible intervention of other species.<sup>11</sup> With the notable exception of **1**, all other ligands and metal complexes discussed in the following exhibit the expected  $\text{C}_{2v}$  symmetry by NMR.

The Pt complex **2** was characterized by  $^1\text{H}$ ,  $^{19}\text{F}$ , and  $^{13}\text{C}$  NMR (the last was assigned by HSQC and HMBC spectra—see the Experimental Section for details) and elemental analysis. The  $^{19}\text{F}$  NMR spectrum of **2** is quite diagnostic (Figure 1), as the singlet for  $\text{CF}_3$  at  $\delta$  -60.9 in dichloromethane- $d_2$  exhibits coupling to  $^{195}\text{Pt}$  ( $^4J_{\text{Pt-F}} = 4.4$  Hz). The  $^{13}\text{C}$  NMR spectrum of

(26) Buffin, B. P.; Kundu, A. *Inorg. Chem. Commun.* **2003**, *6*, 680–684.

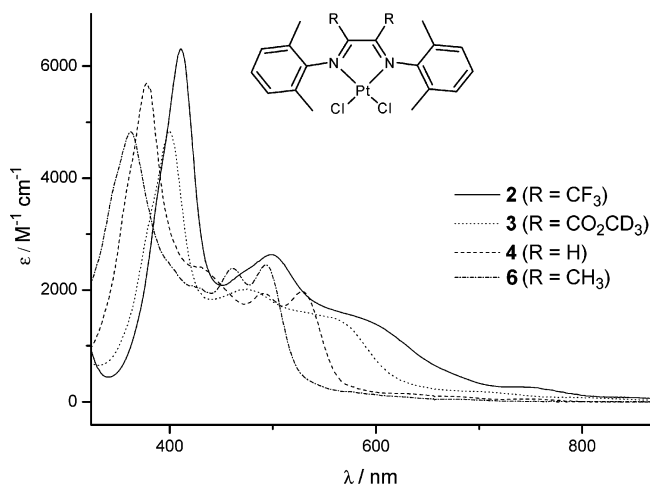


Figure 2. UV-visible spectra for **2–4** and **6** in dichloromethane.

Table 1.  $^{195}\text{Pt}$  NMR Data for (N–N)PtCl<sub>2</sub> Complexes

complex	R	$^{195}\text{Pt}$ ( $\delta$ )
<b>2</b>	$\text{CF}_3$	-1183
<b>3</b>	$\text{COOCD}_3$	-1559
<b>4</b>	H	-2100
<b>6</b>	$\text{CH}_3$	-2179

**2** shows a characteristic quartet from the  $\text{CF}_3$  group due to coupling with fluorine ( $^1J_{\text{C-F}} = 285$  Hz). No Pt satellites were observed in the  $^{13}\text{C}$  NMR spectrum, possibly due to increased chemical shift anisotropy (CSA) at the high field used.<sup>27–31</sup> The imine C resonance at  $\delta$  161.7 is significantly broadened (half-height peak width ca. 100 Hz), due to the proximity of spin-active N, F, and Pt nuclei, but these couplings could not be resolved.

Since **3** was furnished in  $^1\text{H}$  NMR silent methanol- $d_4$ , the identity of this complex with its  $^1\text{H}$  NMR unobservable ester group remained a mystery until the complex was structurally characterized by X-ray diffraction. The ester functionality does, however, show a characteristic IR absorption at  $\nu(\text{CO})$  1753  $\text{cm}^{-1}$ .

The  $^{195}\text{Pt}$  NMR spectra of the metal complexes **2–4** and **6** show a clear trend in their chemical shifts, which correlates with the electron-withdrawing ability of the R groups at the diimine ligand backbone (Table 1). More electron-withdrawing groups result in a downfield shift. The colors of the metal complexes in dichloromethane- $d_2$  solutions are red-purple (**2**, **3**) and orange-red (**4**, **6**), and these differences are manifested in the UV-visible spectra (Figure 2).

**3. Single-Crystal X-ray Crystallography.** X-ray-quality crystals of the fluorinated ligand **1**, which is an oil at ambient temperature, were obtained by storing the pure compound in a freezer at -20 °C. X-ray-quality crystals of **2** and **3** appeared in the NMR-tube reaction mixtures after 6 months and 2 weeks, respectively (see Experimental Section for details). X-ray-quality crystals of **4** were obtained by crystallization from a saturated dichloromethane- $d_2$  solution. Details of the structure determinations are given in the Experimental Section. Table 2 gives experimental and crystallographic data, selected bond distances

(27) Lallemand, J. Y.; Soulie, J.; Chottard, J. C. *J. Chem. Soc., Chem. Commun.* **1980**, 436–438.

(28) Pregosin, P. S. *Coord. Chem. Rev.* **1982**, *44*, 247–291.

(29) Dechter, J. J.; Kowalewski, J. *J. Magn. Reson.* **1984**, *59*, 146–149.

(30) Anklin, C. G.; Pregosin, P. S. *Magn. Reson. Chem.* **1985**, *23*, 671–675.

(31) Skvortsov, A. N. *Russ. J. Gen. Chem.* **2000**, *70*, 1023–1027.

**Table 2.** Crystal Data and Structure Refinement Details for 1–4

	1	2	3	4
formula	C <sub>20</sub> H <sub>18</sub> F <sub>6</sub> N <sub>2</sub>	C <sub>20</sub> H <sub>18</sub> Cl <sub>2</sub> N <sub>2</sub> F <sub>6</sub> Pt	C <sub>22</sub> H <sub>24</sub> Cl <sub>2</sub> N <sub>2</sub> O <sub>4</sub> Pt	C <sub>18</sub> H <sub>20</sub> Cl <sub>2</sub> N <sub>2</sub> Pt · CH <sub>2</sub> Cl <sub>2</sub>
formula wt	400.36	666.36	646.42	615.30
cryst syst	orthorhombic	monoclinic	monoclinic	orthorhombic
color	yellow	black	black	red
space group	<i>Pnna</i>	<i>P2<sub>1</sub>/c</i>	<i>P2<sub>1</sub>/n</i>	<i>Pnna</i>
<i>a</i> /Å	17.3068(10)	8.3808(2)	7.1784(12)	16.485(3)
<i>b</i> /Å	13.2544(8)	12.9274(2)	18.192(3)	18.169(4)
<i>c</i> /Å	8.1088(5)	19.9372(4)	18.014(3)	7.1720(14)
$\alpha$ /deg	90	90	90	90
$\beta$ /deg	90	100.8220(10)	93.953(3)	90
$\gamma$ /deg	90	90	90	90
<i>V</i> /Å <sup>3</sup>	1860.09(19)	2121.62(7)	2346.8(7)	2148.1(7)
<i>Z</i>	4	4	4	4
<i>T</i> /K	105	105	105	105
<i>F</i> (000)	824	1272	1256	1184
radiation	0.710 73	0.710 73	0.710 73	0.710 73
$\theta$ range/deg	2.35–28.29	1.89–40.34	1.59–28.35	2.24–28.31
no. of rflns measd	15 957	36 018	22 632	19 739
no. of unique rflns	2252	13 009	5650	2716
no. of data/restraints/params	1262/0/127	9914/0/280	4679/0/280	2208/0/124
goodness of fit, <i>F</i>	1.1102	1.0891	1.0230	1.0897
R1, wR2 ( <i>I</i> > 3 $\sigma$ ( <i>I</i> ))	0.0434, 0.0478	0.0229, 0.0264	0.0189, 0.0132	0.0152, 0.0174
R1, wR2 (all data)	0.0684, 0.0736	0.0332, 0.0395	0.0239, 0.0138	0.0200, 0.0224
min, max diff peak/e Å <sup>-3</sup>	–0.23, 0.20	–1.54, 3.26	–1.40, 0.89	–0.66, 1.12

**Table 3.** Selected Bond Lengths with Esd's (Å) and Angles (deg) from Crystal Structures of 1–4

	1	2	3	4
Pt–N		1.9962(14)/1.9926(14)	2.0047(13)/1.9984(11)	2.0055(18)
Pt–Cl		2.2767(4)/2.2745(4)	2.2784(5)/2.2832(5)	2.2951(6)
N=C <sub>imine</sub>	1.260(3)	1.307(2)/1.303(2)	1.303(2)/1.298(2)	1.292(3)
N–C <sub>ipso</sub>	1.421(3)	1.449(2)/1.454(2)	1.453(2)/1.454(2)	1.452(3)
C <sub>imine</sub> –C <sub>imine</sub>	1.521(4)	1.469(2)	1.461(2)	1.456(4)
Pt–N=C <sub>imine</sub>		115.9/116.3	115.8/116.1	115.1
Pt–N–C <sub>ipso</sub>		121.6/121.2	121.9/124.2	125.8
N–Pt–N		79.2	78.9	79.2
N–Pt–Cl		96.3/95.8	96.1/95.8	94.6
Cl–Pt–Cl		88.67	89.2	91.6
N=C <sub>imine</sub> –C <sub>imine</sub> =N	54.9	4.7	2.8	0.0
C <sub>imine</sub> =N–C <sub>ipso</sub> –C <sub>ortho</sub> <sup>a</sup>	61.5	83.9/81.8	87.9/86.5	88.4

<sup>a</sup> Torsion angle between mean planes of C<sub>imine</sub>=N–C<sub>ipso</sub> and the aryl group.

and angles for compounds 1–4 are given in Table 3, and Figure 3 gives ORTEP drawings of the structures.

## Discussion

**1. Structural Properties.** When the crystal structure of **1** is compared with the published structure<sup>32</sup> of the analogue that is substituted with CH<sub>3</sub> rather than CF<sub>3</sub> at the imine C's (**5**), several features are particularly noteworthy. What first strikes the eye is that, whereas the structure of **1** is folded (Figure 3), the previously reported structure of **5** is not (both are schematically depicted in Chart 1). The methyl groups at the diimine backbone of **5** are perfectly anti oriented with respect to the central C–C bond, as demonstrated by the 180° N–C–C–N dihedral angle. The aryl and methyl groups at each imine moiety in **5** are cis disposed relative to the C=N bonds (*E* configuration). On the other hand, in **1**—with the somewhat larger CF<sub>3</sub> groups at the backbone—the structure is folded, resulting in what more closely resembles a syn relationship between the trifluoromethyl groups at the backbone (N–C–C–N dihedral angle of 54.9°). The folded structure of **1** leads to obvious  $\pi$ -stacking between the two aryl rings, which is facilitated by the fact that the aryl and CF<sub>3</sub> groups are trans disposed relative to the C=N bonds (but also here with an *E* configuration because of the different

nomenclature priorities of the CH<sub>3</sub> and CF<sub>3</sub> groups). Structural features similar to those of **1** have been seen for related diimines such as ArN=C(CF<sub>3</sub>)C(CF<sub>3</sub>)=NAr (Ar = 4-ClC<sub>6</sub>H<sub>4</sub>,<sup>11</sup> 3,5-(CF<sub>3</sub>)<sub>2</sub>C<sub>6</sub>H<sub>3</sub>,<sup>13</sup>) and ArN=C(Ph)C(Ph)=NAr (Ar = 4-MeC<sub>6</sub>H<sub>4</sub>,<sup>33</sup>). In solution, the observation of two sets of <sup>1</sup>H and <sup>19</sup>F signals of unequal intensities suggests that at least two species with different *E/Z* configurations coexist in solution at ambient temperature (see also the description of even more complex low-temperature spectra in the Results).

Despite the  $\pi$ -stacking and *E* configuration, Sadighi et al. argue that the geometry of these diimines does not preclude metalation to give  $\kappa^2$ (N,N) diimine complexes—for example, *N,N'*-diphenyl-9,10-phenanthrenequinonediimine is readily metalated by (PhCN)<sub>2</sub>PdCl<sub>2</sub>, despite the fact that the free ligand has the “wrong geometry”.<sup>13</sup> The observed problems of metalating ligands with R = CF<sub>3</sub> was rather attributed to the inductive effect of the CF<sub>3</sub> group, which renders the imine N lone pair poorly nucleophilic. This could well explain the great reluctance with which **2** forms in this work.

The C=N bonds in **1** are shorter (by 0.015 Å) and the central C–C bond is longer (by 0.017 Å) in the 1,4-diaza-1,3-butadiene fragment than they are in **5**. This is possibly a result of negative hyperconjugation in **1**,<sup>34,35</sup> stabilizing the C=N bond. A

(32) Kuhn, N.; Steimann, M.; Walker, I. Z. *Kristallogr.: New Cryst. Struct.* **2001**, *216*, 319.

(33) Netland, K. A.; Krivokapic, A.; Tilset, M. Manuscript in preparation.  
(34) Sleigh, J. H.; Stephens, R.; Tatlow, J. C. *J. Chem. Soc., Chem. Commun.* **1979**, 921–922.



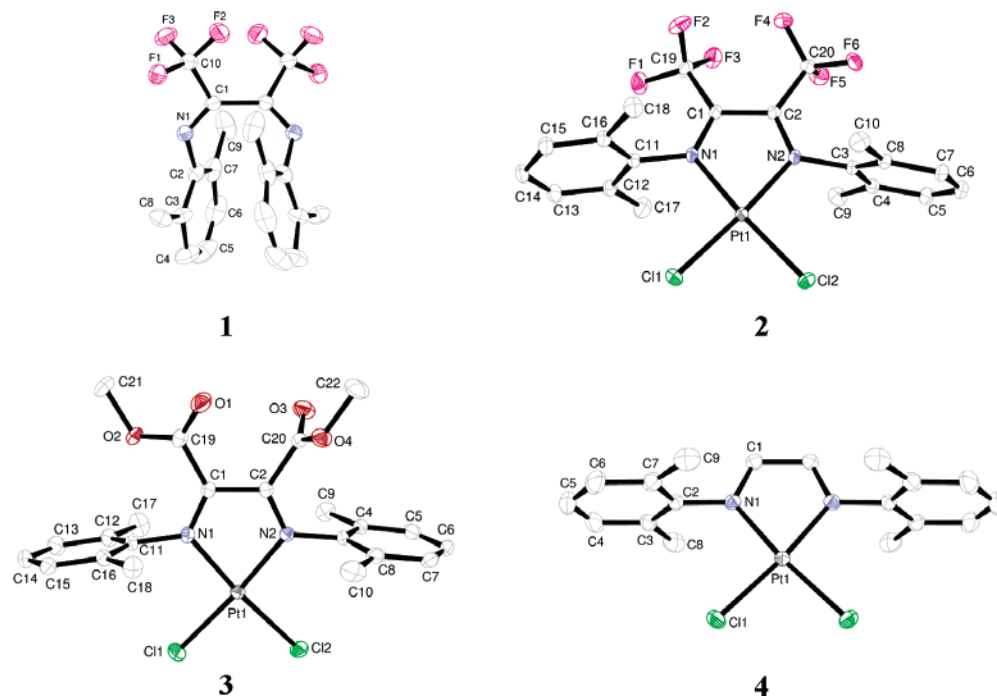
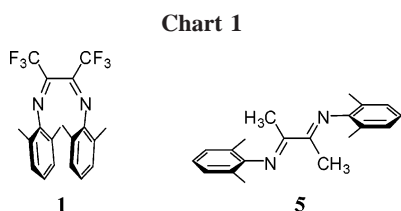


**Figure 3.** ORTEP drawings of **1**–**4**. Ellipsoids are given at the 30% probability level for **1** and the 50% level for **2**–**4**.



comparison of the metric data for **1** and **2** shows that complexation of the diazabutadiene moiety of **1** at PtCl<sub>2</sub> leads to a lengthening of the C=N bonds (by 0.043 and 0.047 Å) and a shortening of the C–C bond (by 0.052 Å). These changes are qualitatively expected, since Pt(II) acts as a good electron donor toward the ligand  $\pi$  system; the ligand LUMO is C=N antibonding and C–C bonding and is particularly prone to accept electron density due to the lowering of the LUMO level by the CF<sub>3</sub> substituents.<sup>9,10</sup>

The changes in metric parameters that occur upon complexation are far from equally pronounced for diimines that are substituted by H or Me at the backbone. Unfortunately, structural data are not available for the free ligand of **4** or of complex **6**. However, if we assume that the metric data for the backbone of ArN=CHCH=NAr (Ar = 2,4,6-Me<sub>3</sub>C<sub>6</sub>H<sub>2</sub>)<sup>36</sup> will be similar to those of the ligand of **4**, it may be inferred that the C=N bond lengthening will be ca. 0.019 Å and the C–C bond shortening ca. 0.007 Å upon complexation of the free ligand of **4** at PtCl<sub>2</sub>. The fact that much greater C–C and C=N bond-distance changes are seen upon complexation of **1** at PtCl<sub>2</sub> underscores the important electronic effects that are introduced by the backbone CF<sub>3</sub> groups.

Thus, the bond alterations induced by the CF<sub>3</sub> groups in **2** clearly emphasize the strong  $\pi$ -acceptor abilities of the diimine ligand **1**. The Pt–N bonds of **2** are slightly shorter than those of **3** and **4**, suggesting a stronger Pt–N interaction. The reduced nucleophilicity of the imine N lone pair arising from the

inductive effect of the CF<sub>3</sub> group therefore appears to be counteracted by the improved  $\pi$ -acceptor properties of the ligand. This observation is contrasted by a comparison of structural data for Tp<sup>Me</sup>PtMe<sub>3</sub> and Tp<sup>(CF<sub>3</sub>)</sup>PtMe<sub>3</sub>. Here, a substantially weaker coordination of the fluorinated Tp ligand is suggested by longer Pt–N bonds and slightly shorter Pt–CH<sub>3</sub> bonds;<sup>37</sup> however, this comparison is less straightforward to interpret, as the TpPt systems are Pt(IV) complexes.

The larger steric bulk of the substituents in the backbones of **2** and **3** (R = CF<sub>3</sub>, CO<sub>2</sub>CD<sub>3</sub>) compared to that in **4** (R = H) is evidenced by the smaller Pt–N–C(ipso) angles in **2** and **3**. The effects of sterically demanding substituents in diimine–Ni(II) complexes for ethene/acrylonitrile copolymerization has recently been studied by Ziegler and co-workers by DFT methods.<sup>38</sup> Substituents such as R = CF<sub>3</sub>, *t*-Bu led to reduced monomer complexation energies. A slight decrease in polymerization activity was calculated for R = CF<sub>3</sub> compared with R = CH<sub>3</sub>. An increased activity was observed by introducing *t*-Bu.

**2. Spectroscopic Properties.** The <sup>195</sup>Pt chemical shift is proportional to and largely determined by the paramagnetic shielding term  $\sigma_{\text{para}}$ .<sup>39,40</sup> This term is proportional to the reciprocal electronic excitation energy  $\Delta E$ . We have recently found that, for a number of neutral diimine Pt(II) complexes, there is a good linear correlation between <sup>195</sup>Pt chemical shifts and the inverse of electronic excitation energies  $\Delta E$ 's obtained from UV–visible spectra or calculated HOMO–LUMO gaps.<sup>41</sup> A similar correlation is seen between <sup>195</sup>Pt chemical shifts of the (N–N)PtCl<sub>2</sub> complexes in this work and the respective  $\lambda_{\text{max}}$  values of the lowest energy UV–vis transitions (Figure 4).  $\lambda_{\text{max}}$  values for **2** and **3** were estimated from the broad shoulders. As expected for an MLCT transition, the electron-withdrawing groups lead to red-shifted  $\lambda_{\text{max}}$  values. Smaller  $\Delta E$ 's (greater  $\lambda$

(37) Fekl, U.; van Eldik, R.; Lovell, S.; Goldberg, K. I. *Organometallics* **2000**, *19*, 3535–3542.

(38) Szabo, M. J.; Galea, N. M.; Michalak, A.; Yang, S. Y.; Groux, L. F.; Piers, W. E.; Ziegler, T. *J. Am. Chem. Soc.* **2005**, *127*, 14692–14703.

(39) Ramsey, N. F. *Phys. Rev.* **1950**, *78*, 699–703.

(40) Griffith, J. S.; Orgel, L. E. *Trans. Faraday Soc.* **1957**, *53*, 601–606.

(41) Lersch, M.; Swang, O.; Tilset, M. Manuscript in preparation.

(35) Dawson, W. H.; Hunter, D. H.; Willis, C. J. *J. Chem. Soc., Chem. Commun.* **1980**, 874–875.

(36) Müller, T.; Schrecke, B.; Bolte, M. *Acta Crystallogr., Sect. E* **2003**, *E59*, o1820–o1821.

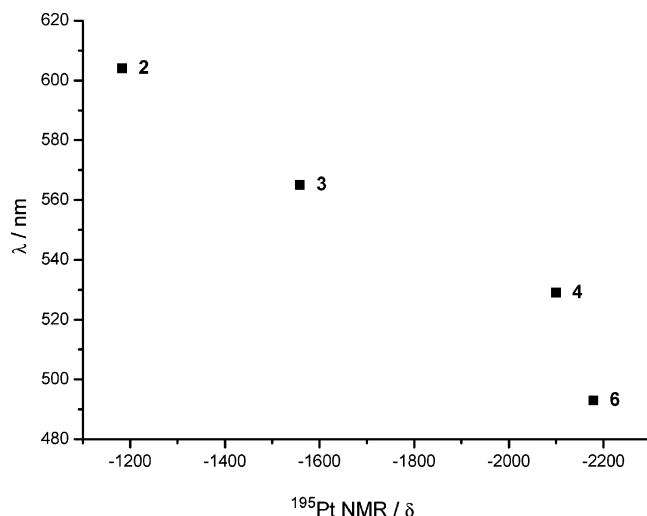


**Figure 4.** Plot of  $\lambda_{\text{max}}$  vs  $^{195}\text{Pt}$  chemical shifts of **2–4** and **6**.

values) should lead to increased chemical shifts,<sup>39,40</sup> as observed. When the backbone R group is changed from  $\text{CF}_3$  via  $\text{CO}_2\text{CD}_3$  and H to  $\text{CH}_3$ , a substantial 1000 ppm upfield shift is seen for  $\delta(^{195}\text{Pt})$ . In comparison, chemical shifts change by less than 100 ppm when substituents at the N-aryl groups are changed from 4- $\text{CF}_3$  to 4- $\text{CH}_3$ .<sup>41</sup> Thus, electronic tuning of the diimine properties is greatly facilitated by backbone substitution, due to the closer proximity of these substituents to Pt.

### Conclusion

The fluorinated  $\alpha$ -diimine Pt(II) complex **2** can be prepared by thermal and photochemical routes. The simplest procedure involves heating the ligand **1** with  $\text{PtCl}_2$  in chlorobenzene at reflux for 3 days. Conveniently, the starting materials can be recovered and reused. The structural features of **2** corroborate the notion that the metal complex is quite electron deficient.  $^{195}\text{Pt}$  chemical shifts of **2–4** and **6** span a range of nearly 1000 ppm and correlate well with  $\lambda_{\text{max}}$  values from UV spectra.

### Experimental Section

**General Considerations.** In the following section, Ar is an abbreviation for the 2,6-dimethylphenyl group. Zeise's salt and  $\text{PtCl}_2$  were purchased from Strem Chemicals and Alfa Aesar, respectively. All reagents were used as received.  $(\text{PhCN})_2\text{PtCl}_2$ ,<sup>42</sup> the diimine complex **6**,<sup>43</sup> and the ligands **1**<sup>11</sup> and  $\text{ArN}=\text{CHCH}=\text{NAr}^1$  were synthesized according to the published procedures. The UV light source was of the type typically used to analyze TLC plates, with an output of approximately 8 W and  $\lambda \sim 355$  nm (the glass in the irradiated NMR tubes/vials effectively blocks radiation with  $\lambda < 300$  nm). Samples were situated approximately 15 cm from the lamp. NMR spectra were recorded on Bruker DPX200, DRX500, and AV II 600 instruments (200 and 500 MHz for  $^1\text{H}$ , 150 MHz for  $^{13}\text{C}$ , 188 MHz for  $^{19}\text{F}$ , 107 MHz for  $^{195}\text{Pt}$ ).  $^1\text{H}$  and  $^{19}\text{F}$  NMR chemical shifts ( $\delta$ ) are reported in ppm relative to TMS via  $\text{CH}_2\text{Cl}_2$  at 5.32 ppm,  $\text{CD}_2\text{Cl}_2$  at 53.8 ppm,  $\text{CH}_2\text{D}_2\text{O}$  at 3.30 ppm, and  $\text{CFCl}_3$  at 0 ppm.  $^{195}\text{Pt}$  NMR chemical shifts are reported in ppm and referenced relative to TMS using  $\Xi_{\text{Pt}} = 21.496\,784$  as recommended by IUPAC.<sup>44</sup> All chemical shifts are reported such that lower frequencies give more negative shifts.  $^{195}\text{Pt}$  NMR spectra were acquired and processed as previously described.<sup>43</sup> IR spectra were

recorded on a Perkin-Elmer One or a Nicolet Magna-IR 550 spectrometer. UV–visible spectra were recorded on an Agilent 8452A spectrophotometer and are reported as  $\lambda_{\text{max}}/\text{nm}$  ( $\epsilon \times 10^{-3}/(\text{M}^{-1} \text{cm}^{-1})$ ).  $\lambda_{\text{max}}$  values estimated from shoulders are marked with sh. Mass spectra were recorded on a ProSpecQ instrument with EI. MS data are given as  $m/z$  (relative intensities, fragment). Elemental analyses were performed by Ilse Beetz Mikroanalytisches Laboratorium, Kronach, Germany. All reactions involving metal complexes were conducted under an atmosphere of  $\text{N}_2$ .

**[ArN=C(CF<sub>3</sub>)C(CF<sub>3</sub>)=NAr]PtCl<sub>2</sub> (2).** **Method A: Thermal, Preparative Scale from PtCl<sub>2</sub>.**  $\text{PtCl}_2$  (15.1 mg, 56.8  $\mu\text{mol}$ ) and **1** (20.0 mg, 50.0  $\mu\text{mol}$ ) in 1 mL of chlorobenzene were stirred at reflux (140 °C) under nitrogen for 3 days. After evaporation of the solvent, the residue was washed with pentane (3  $\times$  3 mL) to remove excess ligand (17.6 mg, 88% recovered). The residue was dissolved in dichloromethane and centrifuged. The precipitated  $\text{PtCl}_2$  (12.8 mg, 85% recovered) was washed twice with dichloromethane. The organic phases were combined, 5% heptane was added to facilitate better powder formation, and the solvents were removed in vacuo to yield pure **2** as a black powder (3.6 mg, 11%). The recovered ligand and  $\text{PtCl}_2$  were resubmitted to the aforementioned reaction conditions, yielding more **2** after 3 days (2.7 mg), resulting in an overall yield of 19% and a new portion of recovered, unreacted starting materials.  $\delta_{\text{H}}$  (200 MHz,  $\text{CD}_2\text{Cl}_2$ ): 2.320 (12H, s, Ar  $\text{CH}_3$ ), 7.21–7.37 (6H, m, Ar H).  $\delta_{\text{H}}$  (200 MHz,  $\text{CD}_3\text{OD}$ ): 2.356 (12H, s, Ar  $\text{CH}_3$ ), 7.20–7.28 (6H, m, Ar H).  $\delta_{\text{C}}$  (150 MHz,  $\text{CD}_2\text{Cl}_2$ ): 18.0 (Ar  $\text{CH}_3$ ), 119.9 (q,  $^1J_{\text{C-F}} = 285$  Hz, N=CCF<sub>3</sub>), 128.0 ( $C_{\text{meta}}$ ), 129.6 ( $C_{\text{ortho}}$ ), 129.9 ( $C_{\text{para}}$ ), 146.1 ( $C_{\text{ipso}}$ ), 161.7 (br, N=CCF<sub>3</sub>).  $\delta_{\text{F}}$  (188 MHz,  $\text{CD}_2\text{Cl}_2$ ): -60.9 ( $^4J_{\text{Pt-F}} = 4.4$  Hz).  $\delta_{\text{F}}$  (188 MHz,  $\text{CD}_3\text{OD}$ ): -60.5.  $\delta_{\text{Pt}}$  (107 MHz,  $\text{CD}_2\text{Cl}_2$ ): -1183.  $\lambda_{\text{max}}$  ( $\text{CH}_2\text{Cl}_2$ ): 411 (6.3), 498 (2.6), 603 sh (1.4).  $m/z$  (EI): 630 (15,  $\text{M}^+ - \text{HCl}$ ), 593 (16,  $\text{M}^+ - 2\text{HCl}$ ), 524 (49), 385 (63), 200 (100).  $m/z$  (EI): found for  $\text{C}_{20}\text{H}_{17}\text{N}_2\text{F}_6\text{Cl}^{194}\text{Pt}$ , 628.0603 ( $\text{M}^+ - \text{HCl}$ ); calcd, 628.0611 (1.2 ppm). Anal. Calcd for  $\text{C}_{20}\text{H}_{18}\text{Cl}_2\text{F}_6\text{N}_2\text{Pt}$ : C, 36.05; H, 2.72; N 4.20. Found: C, 35.98; H, 3.19; N, 4.13.

**Method B: Photochemical, NMR-Tube Scale from Zeise's Salt.** Zeise's salt (3.2 mg, 8.3  $\mu\text{mol}$ ) and **1** (2.0 mg, 5.0  $\mu\text{mol}$ ) were dissolved in 0.7 mL of methanol- $d_4$ . After irradiation with the chromatography UV lamp (20 h), the NMR tube was left to stand in the dark. After 15 weeks, dark crystals of **2** had formed (ca. 1.6 mg, 48%).

**[ArN=(CO<sub>2</sub>CD<sub>3</sub>)C(CO<sub>2</sub>CD<sub>3</sub>)=NAr]PtCl<sub>2</sub> (3).** Zeise's salt (19.6 mg, 50.7  $\mu\text{mol}$ ) and **1** (5.6 mg, 14.0  $\mu\text{mol}$ ) were dissolved in 700  $\mu\text{L}$  of methanol- $d_4$  and transferred to a NMR tube. The reaction mixture was irradiated by UV light, and the reaction was monitored by NMR. After 2 weeks the ligand was consumed, the color of the solution turned lighter, and thin, dark crystals appeared. Crystals suitable for X-ray diffraction were collected. The solvent was evaporated, and the residue was washed with pentane and ether, dissolved in dichloromethane, and filtered through glass wool in a pipet. Evaporation of the solvent yielded **3** as a dark purple powder (4.0 mg, 44%).  $\delta_{\text{H}}$  (200 MHz,  $\text{CD}_2\text{Cl}_2$ ): 2.324 (12H, s, Ar  $\text{CH}_3$ ), 7.16–7.35 (6H, m, Ar H).  $\delta_{\text{H}}$  (200 MHz,  $\text{CD}_3\text{OD}$ ): 2.321 (12H, s, Ar  $\text{CH}_3$ ), 7.15–7.34 (6H, m, Ar H).  $\delta_{\text{Pt}}$  (107 MHz,  $\text{CD}_2\text{Cl}_2$ ): -1559.  $\lambda_{\text{max}}$  ( $\text{CH}_2\text{Cl}_2$ ): 400 (4.8), 475 (2.0), 566 sh (1.4).  $\nu_{\text{max}}$  ( $\text{CH}_2\text{Cl}_2$ )/ $\text{cm}^{-1}$ : 1753 (CO).

**[ArN=HCH=NAr]PtCl<sub>2</sub> (4).** Zeise's salt (113.8 mg, 294.3  $\mu\text{mol}$ ) was dissolved in 2 mL of methanol at 0 °C, the free ligand  $\text{ArN}=\text{CHCH}=\text{NAr}$  (85.6 mg, 323.7  $\mu\text{mol}$ ), dissolved in 4 mL of methanol, was added, and the reaction was stirred at 0 °C for 30 min and another 3 h at room temperature. The precipitate was isolated using a microfiltration kit and washed with methanol/ether. The solid was then dissolved in 100 mL of dichloromethane and the solution refluxed for 1 h. Cooling in a refrigerator produced dark orange microcrystals of **4**, and evaporation of the supernatant produced **4** as a dark orange powder (65.7 and 24.3 mg, respectively, 58% total yield).  $\delta_{\text{H}}$  (200 MHz,  $\text{CD}_2\text{Cl}_2$ ): 2.33 (12H, s, Ar

(42) Anderson, G. K.; Lin, M. *Inorg. Synth.* **1990**, *28*, 60–63.

(43) Wong-Foy, A. G.; Henling, L. M.; Day, M.; Labinger, J. A.; Berzac, J. E. *J. Mol. Catal. A: Chem.* **2002**, *189*, 3–16.

(44) Harris, R. K.; Becker, E. D.; Cabral De Menezes, S. M.; Goodfellow, R.; Granger, P. *Pure Appl. Chem.* **2001**, *73*, 1795–1818.

$CH_3$ ), 7.20–7.35 (6H, m, Ar H), 8.80 (2H, s,  $^3J_{Pt-H} = 97$  Hz, C=NH).  $\delta_{Pt}$  (107 MHz, DMSO- $d_6$ ): –2100. Anal. Calcd for  $C_{18}H_{20}Cl_2N_2Pt$ : C, 40.76; H, 3.80; N, 5.28. Found: C, 40.11; H, 3.55; N, 5.14.  $\lambda_{max}$  ( $CH_2Cl_2$ ): 378 (5.7), 491 (1.9), 528 (2.0).

[ArN=C(Me)C(Me)=NAr]PtCl<sub>2</sub> (**6**). Complex **6** was synthesized according to the published procedure from Zeise's salt and **5**.<sup>44</sup>  $\delta_{Pt}$  (107 MHz, DMSO- $d_6$ ): –2179.  $\lambda_{max}$  ( $CH_2Cl_2$ ): 362 (4.8), 460 (2.4), 493 (2.4).

**X-ray Crystallographic Structure Determination of 1–4.** Storing **1** in the form of an orange oil in a freezer at –20 °C resulted in the formation of crystals after a couple of weeks. Crystals of **2** were collected from an NMR tube initially containing ligand **1** and Zeise's salt in methanol- $d_4$  after approximately 6 months on the lab bench (i.e., method B above, only with ambient light). Continuous irradiation of Zeise's salt and **1** in methanol- $d_4$  for 2 weeks produced crystals of **3**. Crystals of **4** were grown by crystallization from saturated dichloromethane. The crystals were mounted on glass fiber with perfluoro polyether, and the data were collected at 105 K on a Siemens 1K SMART CCD diffractometer using graphite-monochromated Mo K $\alpha$  radiation. Data collection method:  $\omega$ -scan, range 0.3°, crystal to detector distance 5 cm. Data reduction and cell determination were carried out with the SAINT and XPREP<sup>45</sup> programs. Absorption corrections were applied by the use of the SADABS<sup>46</sup> program. All of the structures were solved

(45) SMART and SAINT Area-Detector Control and Integration Software; Siemens Industrial Automation, Inc., Madison, WI, 1995.

(46) SADABS Area-Detector Absorption Correction; Siemens Industrial Automation, Inc., Madison, WI, 1996.

(47) Altomare, A.; Cascarano, G.; Giacovazzo, C.; Guagliardi, A.; Burla, M. C.; Polidori, G.; Camalli, M. *J. Appl. Crystallogr.* **1994**, *27*, 435.

using the Sir92<sup>47</sup> or Sir97<sup>48</sup> programs and refined on  $F$  using the program Crystals.<sup>49</sup>

The non-hydrogen atoms were refined with anisotropic thermal parameters; the H atoms were all located in a difference map, but those attached to carbon atoms were repositioned geometrically. The H atoms were initially refined with soft restraints on the bond lengths and angles to regularize their geometry (C–H in the range 0.93–0.98 Å) and isotropic thermal parameters ( $U(H)$  in the range  $1.2\text{--}1.5 \times U_{equiv}$  of the adjacent atom), after which they were refined with riding constraints. Table 2 gives the experimental and crystallographic data. Selected bond lengths, bond angles, and torsion angles are given in Table 3. Crystallographic data for all four compounds may be obtained as individual CIF files in the Supporting Information.

**Acknowledgment.** We gratefully acknowledge the Norwegian Research Council (NFR) for generous stipends to M.L. and A.K., Osamu Sekiguchi for help with translation of a Japanese patent<sup>12</sup> and recording of MS spectra, Dirk Petersen for recording <sup>13</sup>C, HSQC and HMBC spectra of **2** on a Bruker AV II 600 instrument financed by the NFR, and the NMR steering committee for allowing the instrument to be used for this study.

**Supporting Information Available:** CIF files giving crystallographic data for **1–4**. This material is available free of charge via the Internet at <http://pubs.acs.org>.

OM060897U

(48) Altomare, A.; Burla, M. C.; Camalli, M.; Cascarano, G. L.; Giacovazzo, C.; Guagliardi, A.; Moliterni, A. G. G.; Polidori, G.; Spagna, R. *J. Appl. Crystallogr.* **1999**, *32*, 115–119.

(49) Betteridge, P. W.; Carruthers, J. R.; Cooper, R. I.; Prout, K.; Watkin, D. J. *J. Appl. Crystallogr.* **2003**, *36*, 1487.